High-Throughput Graphene Synthesis in Gapless Stacks

Ya-Ping Hsieh,*,[†] Ching-Hua Shih,[†] Yi-Jing Chiu,[†] and Mario Hofmann[‡]

[†]Graduate Institute of Opto-Mechatronics, National Chung Cheng University, 168 University Road, Min-Hsiung Township, Chiayi County, Taiwan 62102

[‡]Department of Material Science and Engineering, National Cheng Kung University, Tainan, Taiwan 70101

ⓈSupporting Information

Graphene is a monatomic sheet that is expected to find application in many fields ranging from corrosion protection[1,2] and electronic devices[3,4] to transparent conductors.[5,6] Commercial realization of these uses will require scaling of high quality graphene production to square-meter size.[7]

Chemical vapor deposition (CVD) has shown the potential to produce graphene with controllable layer numbers and high performance,[8] but scaling to application-relevant dimensions remains a challenge.

Previously proposed roll-to-roll schemes[5,9,10] are not easily adaptable to the long graphene growth durations that are required to produce high quality material[11] and incur prohibitively large operation cost. Batch CVD processing, which is a mature industrial process, on the other hand, suffers from the limited packing density of samples within the CVD reactor and an 8 × 39 in. reactor chamber is required to produce a 30 in. graphene sheet.[5]

An increase of the sample packing density in traditional CVD is hindered by uniformity issues that arise when sample−sample distances are decreased below length scales in the order of the mean free path of gas.[12] Graphene, on the other hand, might not experience such limitations due to its distinctive growth process. Graphene is commonly synthesized on catalytic substrates with low carbon solubility such as Cu, Ru or Pt[13] resulting in a surface-bound growth mechanism. Furthermore, the substrate's catalytic activity is significantly reduced by graphene coverage causing a self-limiting growth process.[14] The similarity of this growth condition to atomic layer deposition (ALD) techniques raises the expectation that uniform graphene could be grown in confined conditions.[15] Furthermore, such findings could be applied to the scalable production of related 2D materials that grow by surface-bound nucleation and exhibit self-limiting growth such as BN[16] or WSe$_2$.[17]

We here demonstrate the high-throughput growth of graphene on closely stacked substrates. We employ gaps with dimensions that are significantly smaller than the mean free path of gas atoms, resulting in a molecular flow regime[18] that is characterized by Knudsen numbers in excess of 100. The confined conditions were found to yield uniform graphene throughout the stack and within each gap through a self-limiting nucleation process. This characteristic furthermore results in an increased graphene quality compared to traditional growth processes.

The potential of our high density growth process was shown by producing 280 cm^2 of graphene in a common 1 in. furnace which represents a 20-fold increase in production scale.

Graphene was grown by chemical vapor deposition on catalytic Cu substrates following previous reports.[1] Briefly, copper foil (99.8%, Alfa-Aesar, no. 13382) was electropolished before growth in a 1 in. clamshell furnace (Figure 1a,b) and then annealed at 1000 °C in a hydrogen flow of 200 sccm for 30 min. Graphene growth was initiated by introducing 10 sccm CH$_4$ at a pressure of 8 Torr and growth durations were chosen to be 6 h. The grown samples were cooled down to room temperature in a 10 sccm flow of hydrogen.

Transfer using poly(methyl methacrylate) (PMMA, Microchem A9) was conducted following established procedures.[19]

Sheet resistance and macroscopic Hall-effect mobility was measured on 1 × 1 cm graphene samples located on Si wafers with a 300 nm thick thermal oxide by a 4-point probe in van der Pauw geometry using silver ink as contacts. Raman measurements were performed in a home-built Micro-Raman system employing a 532 nm laser excitation source. 10 Raman spectra were analyzed and averaged for each sample to obtain I_D/I_G and I_{2D}/I_G. Image processing was used to analyze the coverage, grain density and grain size.

We assembled close-packed stacks by alternating copper foil and a refractory film to prevent the sticking of neighboring copper foils. The spacer material was chosen to be graphite (SGL Sigraflex) due to its inert nature and high melting point but other refractory materials were shown to work, as well (see Figure S2). Control experiments ensure that graphene growth was not caused by the graphite layers (Figure S2). Fused silica slides (23 × 75 × 2 mm, Xide Technology Ltd.) were used as bottom and top caps of the stack (Figure 1b).

Figure 1c shows a stack of 20 copper foil pieces (2 × 7 cm) separated from each other by graphite foil (Figure 2a). The resulting stack is ~10 mm tall and weighs ~20 g. The height and weight raise concerns about the uniformity of temperature, flow conditions and contact pressure for samples at different positions of the assembly. To investigate this issue, we transferred graphene from different Cu layers in the stack (Figure 2a). The low Raman I_D/I_G ratio (~0.03) confirms the high quality of the graphene and the high Raman I_{2D}/I_G ratio (~2.3) suggests the predominance of single-layer graphene (Figure 2b).[20] More importantly, the variation of each parameter across the stack is less than 13% and shows no trend (Figure 2c). The high extracted average Hall mobility
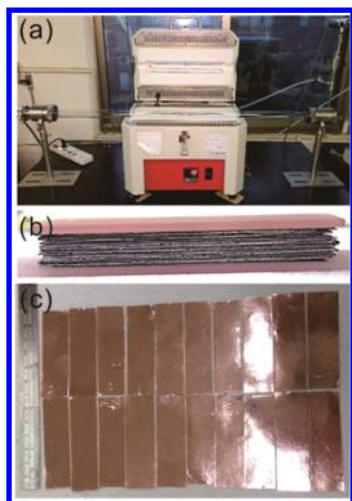
Figure 1. Depiction of growth setup: (a) photographs of 1″ CVD setup, (b) photograph of gapless growth assembly, (c) photograph of amount of Cu foil grown in one run.
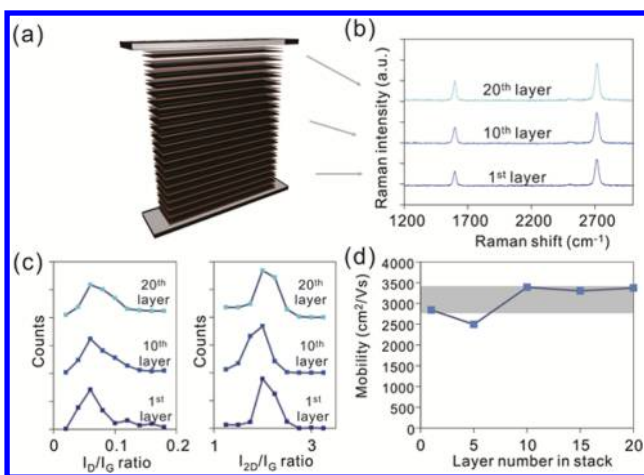
Figure 2. Vertical uniformity of graphene properties within stack: (a) illustration of stack position, (b) representative Raman spectra of 3 layers, (c) histogram of I_D/I_G ratios for 3 layers, (c) histogram of I_{2D}/I_G ratio for 3 layers, (d) graphene Hall mobility for different layers.

Figure 3. Horizontal growth process (a) coverage vs position along one pore for various growth durations, (inset) extracted values of $(4Dt)^{1/2}$ vs $\sqrt{t}$, (b) distribution of grain size and grain density along one pore, (c) photographs of graphene grown at the edge and the center of on copper foil.

($\sim$3083 cm^2/(V·s)) and the low variability further corroborates the high and uniform quality of graphene across the stack.

This result indicates that the quality of graphene within the stack is not affected by variations in temperature or pore size. The remarkable robustness of the graphene growth raises questions about the growth process.

To investigate the growth process, we characterized the graphene morphology along one copper foil within the stack. Because of the direct contact between the graphite and the copper layer, confinement effects occur. AFM measurements detect a finite roughness of the two contacting layers (R_a^{Cu} = 70 nm, $R_a^{Graphite}$ = 79 nm), which facilitates gas transport but flow restrictions occur akin to flow in a pore with an aspect ratio above 10^5. In this regime, molecular flow is expected to occur, which is characterized by the significant contribution of wall collisions on the mass transport.[18] The importance of confinement effects on the graphene growth can be inferred from the evolution of the graphene distribution with time. Figure 3a shows the graphene coverage along a 7 cm long copper foil. At short growth durations, the center shows a

smaller coverage; long growth durations lead to uniform coverage along the whole sample.

The spatial and temporal change of the graphene coverage has been previously found to be proportional to the concentration of carbon precursors in the transport-controlled regime of the present CVD process.[14] We approximate the precursor concentration with a superposition of two half-space solutions originating from the edges of the sample.

$$c(x, t) = c_0\left(\text{erfc}\left(\frac{x - x_{b1}}{\sqrt{4Dt}} \right) + \text{erfc}\left(-\frac{x - x_{b2}}{\sqrt{4Dt}} \right) \right)$$

where c_0 is the concentration of gas concentration outside of the stack, x_{b1} and x_{b2} are the positions of the copper foil edges, and $(4Dt)^{1/2}$ was chosen as a fitting parameter for each curve and used to extract the diffusion coefficient D (inset of Figure 3a).

The observed excellent agreement between the coverage evolution and the concentration distribution validates our model and fitting allows us to extract the diffusion coefficient of the gas transport. We obtain a value of $D = 1.5 \times 10^{-7}$ m^2/s, which is approximately 3 orders of magnitude smaller than the diffusion coefficient of CH$_4$.[21] This decreased diffusivity is due to the confinement effects and can be approximated by

$$D = D_0/Kn$$

where D_0 is the free-space diffusivity and Kn is the Knudsen number that represents the ratio of the mean free path and the system size.[18] The growth conditions in our system yield an approximate gas mean free path λ = 25 μm and the pore size is associated with the substrate roughness ($d \sim$ 150 nm). These

parameters result in a Knudsen number of $Kn = 166$ and the corresponding lowered diffusion coefficient is in agreement with our observation.

The effect of the decreased efficiency of mass transport in the molecular flow regime is illustrated when analyzing the graphene morphology along the copper foil (Figure 3c,d. The irregular shape of the graphene grains indicates a hydrogen-starved growth condition.[22] A pronounced minimum in the grain size can be seen in the center of the sample (Figure 3(b). This behavior indicates a transport-controlled growth process that occurs when the supply of carbon is slower than its conversion into graphene.

In the observed diffusion-controlled transport regime, the partial pressure of precursor should vary significantly with position. One important observation is the absence of a variation of nucleation density with position (Figure 3b) indicating a self-limiting nucleation process that is independent of growth conditions.

This behavior is thought to be due to the combination of a confinement-induced decrease in nucleation seeds[23] and a concentration of precursor below the critical threshold of adsorption-controlled nucleation kinetics.[24]

Our observation of a constant nucleation density suggests that the graphene morphology is not depending on the growth position because both graphene grain density and final dimensions are controlled by the nucleation density through a self-limiting nucleation and a self-limiting growth process.

This conclusion is supported by the observed uniformity of graphene quality along the pore. Raman characterization, electrical measurements and transmittance measurements all demonstrate variation of less than 10% between graphene samples grown across one copper foil stack within the stack (Figure 4).
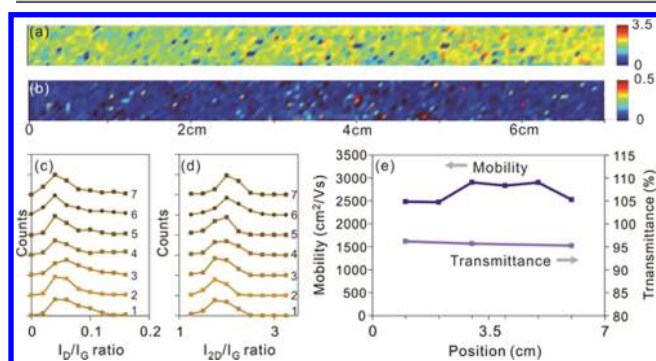
Figure 4. Uniformity of properties along one graphene layer within the stack (a) Raman map of I_D/I_G ratio, (b) Raman map of I_{2D}/I_G ratio, (c,d) histograms of I_D/I_G ratio (c) and I_{2D}/I_G ratio (d) at various positions along graphene layer, (e) analysis of carrier mobility and transmittance.

The advantages of the observed self-limiting nucleation process are further illustrated by comparing our results to unconfined growth under identical conditions. For this purpose, an uncovered Cu layer was included in the covered graphene growth process described above. We observe a decrease of nucleation density by 90% for confined conditions (Figure S5), suggesting that confinement is necessary to achieve self-limiting nucleation conditions. A lower defectiveness of the graphene grown under confined conditions is indicated by a 30% decrease in Raman I_D/I_G ratio. This change in Raman features had been associated with a decreased density

of grain boundaries.[25] The decreased defectiveness is further confirmed by a 15% improvement in resistance to etching that is thought to originate from a decrease in structural defects in the graphene basal plane.[26] The lower density of polycrystalline grains and grain boundaries results in enhanced carrier transport within the graphene film and improvements in carrier mobility and sheet resistance by 40% were observed, yielding a large-scale (1 cm^2) Hall-effect mobility of 3349 cm^2/(V·s) and sheet resistance of 460 $\Omega/\square$. These values are among the highest reported mobilities in CVD graphene devices to date.[27,28]

Future studies have to explore the limits of achievable scale. Geometrical considerations suggest that a 1 in. furnace with a 10 cm heating zone could produce 0.3 m^2 graphene, which would be a 300-fold increase in size. Scaling to a 3 in. furnace would improve the yield to 17 m^2 or 3700 three-inch graphene wafers per run.

In conclusion, we have demonstrated the high-throughput production of graphene by CVD using close-packed stacks of gapless and alternating layers of graphite and growth substrates. This arrangement yielded a 20-fold increase in production scale and a higher quality of graphene quality compared to traditional growth results. The origin of this improvement was found to be due to a self-limiting nucleation process originating from confinement effects at the growth-substrate interface. Molecular scale flow conditions resulted in the uniform quality of graphene along the graphite-growth substrate interface and across the stack. Our results provide a novel route toward the large scale synthesis of graphene and related 2D materials for commercial applications.

■ ASSOCIATED CONTENT

Ⓢ Supporting Information

The Supporting Information is available free of charge on the ACS Publications website at DOI: 10.1021/acs.chemmater.5b04007.

> Optical microscope images of graphene grown under methane-free conditions and using other refractory spacers; absorption spectra, Raman spectra, and raw data of electrical measurements (PDF).

■ AUTHOR INFORMATION

Corresponding Author
*Y.-P. Hsieh. E-mail: yphsieh@ccu.edu.tw.
Notes
The authors declare no competing financial interest.

■ ACKNOWLEDGMENTS

■ REFERENCES

(1) Hsieh, Y.-P.; Hofmann, M.; Chang, K.-W.; Jhu, J. G.; Li, Y.-Y.; Chen, K. Y.; Yang, C. C.; Chang, W.-S.; Chen, L.-C. Complete corrosion inhibition through graphene defect passivation. *ACS Nano* **2014**, *8*, 443−448.

(2) Zhou, F.; Li, Z.; Shenoy, G. J.; Li, L.; Liu, H. Enhanced room-temperature corrosion of copper in the presence of graphene. *ACS Nano* **2013**, *7*, 6939−6947.

(3) Hsieh, Y.-P.; Yen, C.-H.; Lin, P.-S.; Ma, S.-W.; Ting, C.-C.; Wu, C.-I.; Hofmann, M. Ultra-high sensitivity graphene photosensors. *Appl. Phys. Lett.* **2014**, *104*, 041110.

(4) Wang, Y.; Shi, Z.; Huang, Y.; Ma, Y.; Wang, C.; Chen, M.; Chen, Y. Supercapacitor devices based on graphene materials. *J. Phys. Chem. C* **2009**, *113*, 13103−13107.

(5) Bae, S.; Kim, H.; Lee, Y.; Xu, X.; Park, J. S.; Zheng, Y.; Balakrishnan, J.; Lei, T.; Kim, H. R.; Song, Y. I.; Kim, Y. J.; Kim, K. S.; Ozyilmaz, B.; Ahn, J. H.; Hong, B. H.; Iijima, S. Roll-to-roll production of 30-in. graphene films for transparent electrodes. *Nat. Nanotechnol.* **2010**, *5*, 574−578.

(6) De, S.; Coleman, J. N. Are there fundamental limitations on the sheet resistance and transmittance of thin graphene films? *ACS Nano* **2010**, *4*, 2713−2720.

(7) Zurutuza, A.; Marinelli, C. Challenges and opportunities in graphene commercialization. *Nat. Nanotechnol.* **2014**, *9*, 730−734.

(8) Reina, A.; Thiele, S.; Jia, X.; Bhaviripudi, S.; Dresselhaus, M. S.; Schaefer, J. A.; Kong, J. Growth of large-area single-and bi-layer graphene by controlled carbon precipitation on polycrystalline Ni surfaces. *Nano Res.* **2009**, *2*, 509−516.

(9) Juang, Z.-Y.; Wu, C.-Y.; Lu, A.-Y.; Su, C.-Y.; Leou, K.-C.; Chen, F.-R.; Tsai, C.-H. Graphene synthesis by chemical vapor deposition and transfer by a roll-to-roll process. *Carbon* **2010**, *48*, 3169−3174.

(10) Kobayashi, T.; Bando, M.; Kimura, N.; Shimizu, K.; Kadono, K.; Umezu, N.; Miyahara, K.; Hayazaki, S.; Nagai, S.; Mizuguchi, Y.; Murakami, Y.; Hobara, D. Production of a 100-m-long high-quality graphene transparent conductive film by roll-to-roll chemical vapor deposition and transfer process. *Appl. Phys. Lett.* **2013**, *102*, 023112.

(11) Zhou, H. L.; Yu, W. J.; Liu, L. X.; Cheng, R.; Chen, Y.; Huang, X. Q.; Liu, Y.; Wang, Y.; Huang, Y.; Duan, X. F. Chemical vapour deposition growth of large single crystals of monolayer and bilayer graphene. *Nat. Commun.* **2013**, *4*, 8.

(12) Cooke, M.; Harris, G. Monte Carlo simulation of thin-film deposition in a rectangular groove. *J. Vac. Sci. Technol., A* **1989**, *7*, 3217−3221.

(13) Seah, C.-M.; Chai, S.-P.; Mohamed, A. R. Mechanisms of graphene growth by chemical vapour deposition on transition metals. *Carbon* **2014**, *70*, 1−21.

(14) Hsieh, Y.-P.; Hofmann, M.; Kong, J. Promoter-assisted chemical vapor deposition of graphene. *Carbon* **2014**, *67*, 417−423.

(15) Elam, J.; Routkevitch, D.; Mardilovich, P.; George, S. Conformal coating on ultrahigh-aspect-ratio nanopores of anodic alumina by atomic layer deposition. *Chem. Mater.* **2003**, *15*, 3507−3517.

(16) Kim, K. K.; Hsu, A.; Jia, X.; Kim, S. M.; Shi, Y.; Hofmann, M.; Nezich, D.; Rodriguez-Nieva, J. F.; Dresselhaus, M.; Palacios, T. Synthesis of monolayer hexagonal boron nitride on Cu foil using chemical vapor deposition. *Nano Lett.* **2012**, *12*, 161−166.

(17) Liu, B.; Fathi, M.; Chen, L.; Abbas, A.; Ma, Y.; Zhou, C. Chemical vapor deposition growth of monolayer WSe_2 with tunable device characteristics and growth mechanism study. *ACS Nano* **2015**, *9*, 6119−6127.

(18) Bong, H.; Jo, S. B.; Kang, B.; Lee, S. K.; Kim, H. H.; Lee, S. G.; Cho, K. Graphene growth under Knudsen molecular flow on a confined catalytic metal coil. *Nanoscale* **2015**, *7*, 1314−1324.

(19) Hofmann, M.; Hsieh, Y.-P.; Hsu, A. L.; Kong, J. Scalable, flexible and high resolution patterning of CVD graphene. *Nanoscale* **2014**, *6*, 289−292.

(20) Jorio, A.; Cançado, L. G. Perspectives on Raman spectroscopy of graphene-based systems: from the perfect two-dimensional surface to charcoal. *Phys. Chem. Chem. Phys.* **2012**, *14*, 15246−15256.

(21) Safron, N. S.; Arnold, M. S. Experimentally determined model of atmospheric pressure CVD of graphene on Cu. *J. Mater. Chem. C* **2014**, *2*, 744−755.

(22) Vlassiouk, I.; Regmi, M.; Fulvio, P.; Dai, S.; Datskos, P.; Eres, G.; Smirnov, S. Role of hydrogen in chemical vapor deposition growth of large single-crystal graphene. *ACS Nano* **2011**, *5*, 6069−6076.

(23) Chen, S. S.; Ji, H. X.; Chou, H.; Li, Q. Y.; Li, H. Y.; Suk, J. W.; Piner, R.; Liao, L.; Cai, W. W.; Ruoff, R. S. Millimeter-size single-crystal graphene by suppressing evaporative loss of Cu during low pressure chemical vapor deposition. *Adv. Mater.* **2013**, *25*, 2062−2065.

(24) Wu, T.; Ding, G.; Shen, H.; Wang, H.; Sun, L.; Jiang, D.; Xie, X.; Jiang, M. Triggering the continuous growth of graphene toward millimeter-sized grains. *Adv. Funct. Mater.* **2013**, *23*, 198−203.

(25) Duong, D. L.; Han, G. H.; Lee, S. M.; Gunes, F.; Kim, E. S.; Kim, S. T.; Kim, H.; Ta, Q. H.; So, K. P.; Yoon, S. J.; Chae, S. J.; Jo, Y. W.; Park, M. H.; Chae, S. H.; Lim, S. C.; Choi, J. Y.; Lee, Y. H. Probing graphene grain boundaries with optical microscopy. *Nature* **2012**, *490*, 235−239.

(26) Hofmann, M.; Shin, Y.; Hsieh, Y.-P.; Dresselhaus, M.; Kong, J. A facile tool for the characterization of two-dimensional materials grown by chemical vapor deposition. *Nano Res.* **2012**, *5*, 504−511.

(27) Kobayashi, T.; Bando, M.; Kimura, N.; Shimizu, K.; Kadono, K.; Umezu, N.; Miyahara, K.; Hayazaki, S.; Nagai, S.; Mizuguchi, Y. Production of a 100-m-long high-quality graphene transparent conductive film by roll-to-roll chemical vapor deposition and transfer process. *Appl. Phys. Lett.* **2013**, *102*, 023112.

(28) Kim, K. K.; Reina, A.; Shi, Y.; Park, H.; Li, L.-J.; Lee, Y. H.; Kong, J. Enhancing the conductivity of transparent graphene films via doping. *Nanotechnology* **2010**, *21*, 285205.